

## Regioselectivity and Activity of Cytochrome P450 BM-3 and Mutant F87A in Reactions Driven by Hydrogen Peroxide

Patrick C. Cirino, Frances H. Arnold\*

Division of Chemistry and Chemical Engineering 210-41, California Institute of Technology, Pasadena, CA 91125, USA  
Fax: (+1)-626-568-8743, e-mail: frances@cheme.caltech.edu

Received: May 14, 2002; Accepted: July 18, 2002

Dedicated to Roger Sheldon on the occasion of his 60th birthday.

**Abstract:** Cytochrome P450 BM-3 (EC 1.14.14.1) is a monooxygenase that utilizes NADPH and dioxygen to hydroxylate fatty acids at subterminal positions. The enzyme is also capable of functioning as a peroxygenase in the same reaction, by utilizing hydrogen peroxide in place of the reductase domain, cofactor and oxygen. As a starting point for developing a practically useful hydroxylation biocatalyst, we compare the activity and regioselectivity of wild-type P450 BM-3 and its F87A mutant on various fatty acids. Neither enzyme catalyzes terminal hydroxylation under any of the conditions studied. While significantly enhancing peroxygenase activity, the F87A mutation also shifts hydroxylation further away from the terminal position. The H<sub>2</sub>O<sub>2</sub>-driven reactions with either the full-length BM-3 enzyme or the heme domain are slow, but yield product distributions very similar to those generated when using NADPH and O<sub>2</sub>.

**Keywords:** cytochrome P450 BM-3; enzyme catalysis; fatty acids; hydroxylation; peroxide shunt pathway; peroxygenase; regioselectivity

Roger Sheldon's track record of combining excellent science with solving problems of practical importance provides a high standard for research in catalysis and biocatalysis. Unfortunately for those of us studying biological systems, 'practical' and 'biocatalytic' are words that rarely sit comfortably in juxtaposition. Nonetheless, we share Roger's hope that more of nature's clean, selective catalysts will be exploited in industrial chemical processes, particularly oxidations.

The cytochromes P450 are heme-containing enzymes that perform key functions in nature by catalyzing monooxygenations on a wide range of substrates. Many of these reactions are difficult to perform by synthetic methods, and there is some interest in using P450s for biocatalytic applications<sup>[1]</sup> as well as notable successes.<sup>[1a,2]</sup> Several years ago we proposed that P450s' ability

to utilize peroxides in place of dioxygen and NAD(P)H to drive hydroxylation via the peroxide "shunt" pathway could provide a way to confront the cofactor regeneration problem.<sup>[3]</sup> However, the P450 peroxygenase reaction is usually very inefficient and the enzyme is rapidly inactivated by the peroxide. We showed that directed evolution by random mutagenesis and high throughput screening could improve the performance of P450cam in the shunt pathway.

Following these studies, we focused on evolving a somewhat more robust starting enzyme, P450 BM-3 from *Bacillus megaterium*,<sup>[4]</sup> into a practical biocatalyst, also by improving its shunt activity. P450 BM-3 hydroxylates fatty acids primarily at positions  $\omega$ -1,  $\omega$ -2, and  $\omega$ -3.<sup>[5]</sup> Residue Phe87 lies close to the heme on the distal side and plays a role in positioning the substrate for oxidation.<sup>[6]</sup> While we were developing an assay to screen for improvements in H<sub>2</sub>O<sub>2</sub>-driven hydroxylation by P450 BM-3, we noted that peroxygenase activity was enhanced by the mutation of this residue to alanine (F87A). This same observation has been reported by Li et al.<sup>[7]</sup>

Our laboratory evolution experiments use a rapid assay on *p*-nitrophenoxycarboxylic acid surrogate substrates ("*p*NCAs") developed by Schwaneberg.<sup>[8]</sup> This assay, which is sensitive to hydroxylation at a fixed position (that leads to release of *p*-nitrophenol), reliably identifies enzymes that utilize peroxides more efficiently (P.C.C. and F.H.A., unpublished results). In addition to knowing how the accumulating mutations affect overall activity, we would like to know how they affect specificity of the enzyme and, in particular, the regioselectivity of hydroxylation. We would also like to know whether the peroxide-driven reaction gives the same product distribution as the reaction using cofactor and oxygen. A particularly attractive feature of P450 catalysis via the shunt pathway is that the reductase domain is no longer needed. However, it is important to determine whether using the hydroxylase domain alone changes the activity or distribution of hydroxylated products.

Here we report regioselectivities and reaction rates for these various permutations of wild-type BM-3 and its F87A mutant acting on myristic (C<sub>14</sub>), lauric (C<sub>12</sub>), and

capric (C<sub>10</sub>) acids. Hydroxylated isomers were identified by GC/MS and quantified using a flame ionization detector, as described in the Experimental Section. Rates of the NADPH-driven reactions were determined by measuring NADPH consumption and NADPH coupling efficiency, while H<sub>2</sub>O<sub>2</sub>-driven reaction rates were estimated by quantifying the products from one-minute reactions. Table 1 summarizes the results from these experiments, and representative GC traces of the derivatized products from reactions with lauric acid are shown in Figure 1. Figure 2 shows representative MS fragmentation patterns for the derivatized ω-3 and ω-5 hydroxylated lauric acid products (9- and 7-hydroxy-lauric acids) corresponding to the peaks at 10.95 min. and 10.55 min., respectively, from Figure 1. All product chromatographic resolutions and fragmentation patterns appeared as expected and are in good agreement with previous reports.<sup>[9]</sup>

The product distributions for NADPH-driven reactions of wild-type with myristic acid and lauric acid agree with what has been reported;<sup>[5]</sup> the products of capric acid hydroxylation have not been reported previously. The rates of NADPH consumption for wild-type with

myristic and lauric acid are also similar to literature values,<sup>[10]</sup> while no rates for capric acid have been previously reported. No significant products other than those reported in Table 1 were detected, including ω-hydroxylation products. NADPH consumption by wild-type BM-3 with myristic acid has been indirectly shown to be tightly coupled to product formation.<sup>[11]</sup> The value we report for the coupling efficiency of wild-type with lauric acid (84%) is similar to that reported by Cowart et al.<sup>[12]</sup> Coupling efficiency for wild-type with capric acid is very low (32%).

The F87A mutation reduces the reaction rate in the NADPH-driven reaction and also reduces the coupling efficiency. Similar results have been reported for the F87V mutant.<sup>[12]</sup> F87A also broadens regioselectivity and shifts hydroxylation away from the terminal position, in contrast to what has been previously reported.<sup>[13]</sup> The primary position of hydroxylation with myristic acid is shifted from ω-1 to ω-5. These results agree with a similar study on the F87V mutant,<sup>[14]</sup> which suggested that replacement of Phe87 with a smaller residue allows for deeper penetration of long-chain substrates into the active site.

**Table 1.** Fatty acid hydroxylation activity of wild-type BM-3 and mutant F87A under the natural pathway (NADPH + O<sub>2</sub>) and the peroxide shunt pathway. BWT: full-length wild-type BM-3. HWT: heme domain wild-type. BFA: full-length F87A mutant. HFA: heme domain F87A. ND: could not be determined. All standard deviations were less than 10% of the average, except for the standard deviations reported below.

| Fatty Acid                     | P450 | Reaction                      | Distribution of Hydroxylated Products [%] |       |       |        |       |        | Initial Rate <sup>[a]</sup> (NADPH Coupling) |
|--------------------------------|------|-------------------------------|---|-------|-------|--------|-------|--------|--|
|                                |      |                               | ω-6                                       | ω-5   | ω-4   | ω-3    | ω-2   | ω-1    |  |
| Myristic<br>(C <sub>14</sub> ) | BWT  | NADPH + O <sub>2</sub>        |   |       | 1     | 24     | 26    | 48     | 1700 <sup>[b]</sup>                          |
|                                | HWT  | H <sub>2</sub> O <sub>2</sub> |   |       |       | 33     | 29    | 38     | ND <sup>[c]</sup>                            |
|                                | BFA  | NADPH + O <sub>2</sub>        | 2   | 57    | 16    | 7      | 8     | 11     | 830 ± 100 (ND)                               |
|                                | BFA  | H <sub>2</sub> O <sub>2</sub> | 5 ± 2                                     | 56    | 14    | 5      | 6     | 15     | ND   |
|                                | HFA  | H <sub>2</sub> O <sub>2</sub> | 4 ± 1                                     | 61    | 13    | 5      | 6 ± 1 | 12     | ND   |
| Lauric<br>(C <sub>12</sub> )   | BWT  | NADPH + O <sub>2</sub>        |   |       |       | 37     | 27    | 36     | 1200 (84%)                                   |
|                                | BWT  | H <sub>2</sub> O <sub>2</sub> |   |       |       | 42     | 28    | 30 ± 4 | ND <sup>[c]</sup>                            |
|                                | HWT  | H <sub>2</sub> O <sub>2</sub> |   |       |       | 46     | 27    | 28 ± 3 | ND <sup>[c]</sup>                            |
|                                | BFA  | NADPH + O <sub>2</sub>        |   | 24    | 19    | 40     | 10    | 6      | 350 ± 50 (67%)                               |
|                                | BFA  | H <sub>2</sub> O <sub>2</sub> |   | 36    | 20    | 29     | 8     | 7 ± 1  | 11   |
|                                | HFA  | H <sub>2</sub> O <sub>2</sub> |   | 39    | 19    | 30     | 7     | 5      | 10   |
| Capric<br>(C <sub>10</sub> )   | BWT  | NADPH + O <sub>2</sub>        |   |       |       | 13     | 19    | 68     | 150 (32%)                                    |
|                                | BWT  | H <sub>2</sub> O <sub>2</sub> |   |       |       | 21 ± 3 | 23    | 56     | ND <sup>[c]</sup>                            |
|                                | HWT  | H <sub>2</sub> O <sub>2</sub> |   |       |       | 18     | 23    | 59     | ND <sup>[c]</sup>                            |
|                                | BFA  | NADPH + O <sub>2</sub>        |   |       |       | 39     | 23    | 38     | 24 (18%)                                     |
|                                | BFA  | H <sub>2</sub> O <sub>2</sub> |   | 3 ± 2 | 5 ± 1 | 48     | 17    | 28     | 34   |
|                                | HFA  | H <sub>2</sub> O <sub>2</sub> |   | 3 ± 1 | 4 ± 1 | 53     | 17    | 23     | 46 ± 8                                       |

<sup>[a]</sup> Rates are reported as mole/mole P450/min. Rates for the NADPH-driven reactions are the initial rates of NADPH consumption, with coupling efficiencies reported in parentheses. Coupling efficiencies were calculated as the total moles of hydroxylated product formed per 100 moles NADPH consumed. Initial rates of H<sub>2</sub>O<sub>2</sub>-driven reactions were estimated by measuring the amount of product formed in one minute.

<sup>[b]</sup> NADPH consumption in this reaction is reported to be tightly coupled to product formation.<sup>[11]</sup>

<sup>[c]</sup> WT was estimated to be capable of only ~2 – 3 turnovers (before complete inactivation) in the peroxide-driven hydroxylation reaction.

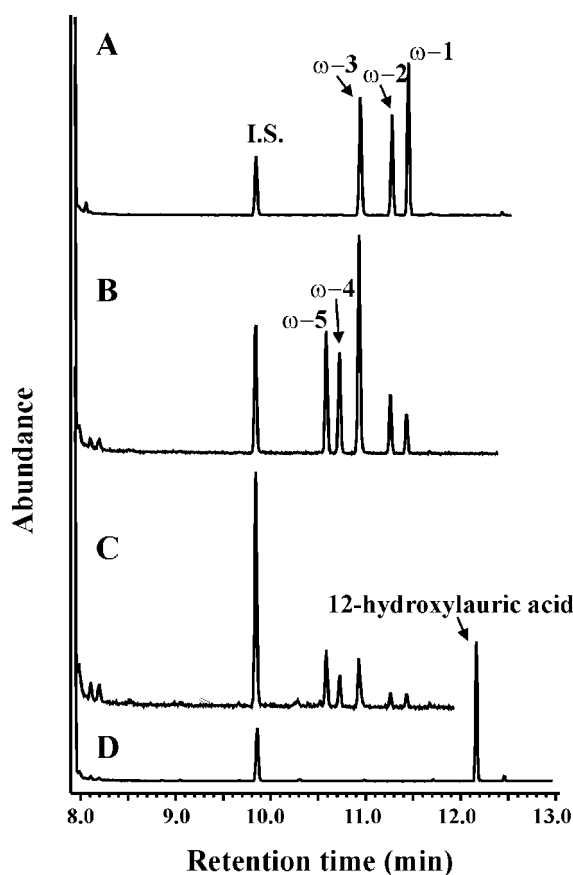


**Figure 1.** Representative chromatogram of the TMS-derivatized hydroxylated products from reactions of P450 BM-3 with lauric acid. **A)** Reaction of wild-type BM-3 with NADPH + O<sub>2</sub>. **B)** Reaction of mutant F87A with NADPH + O<sub>2</sub>. **C)** Reaction of mutant F87A with H<sub>2</sub>O<sub>2</sub>. **D)** 12-Hydroxylauric acid standard. This sample was prepared in the same manner as the reaction samples, except the enzyme was first inactivated. I.S. = internal standard (10-hydroxycapric acid). For quantitative comparisons, all peak areas were normalized relative to the internal standard peak area. Samples were prepared as described in the Experimental Section.

Reactions of P450s with various peroxides have been studied in detail (refer to [15]). Significant differences between products of the NADPH and peroxide pathways have been reported for liver microsomal P450s when organic hydroperoxides were used.[16] In contrast, reactions of microsomal P450s using H<sub>2</sub>O<sub>2</sub> gave products identical to or very similar to those found from the NADPH reactions.[17] We have found that the product distributions for the monooxygenase and H<sub>2</sub>O<sub>2</sub>-driven peroxygenase reactions for purified P450 BM-3 are also very similar. Furthermore, removal of the reductase domain has no significant effect on shunt pathway activity or products. Thus it is likely that the shunt pathway goes through the same active oxidative intermediate(s). The small shift in product distribution for the peroxygenase reaction could reflect slight variations in substrate placement due to the presence

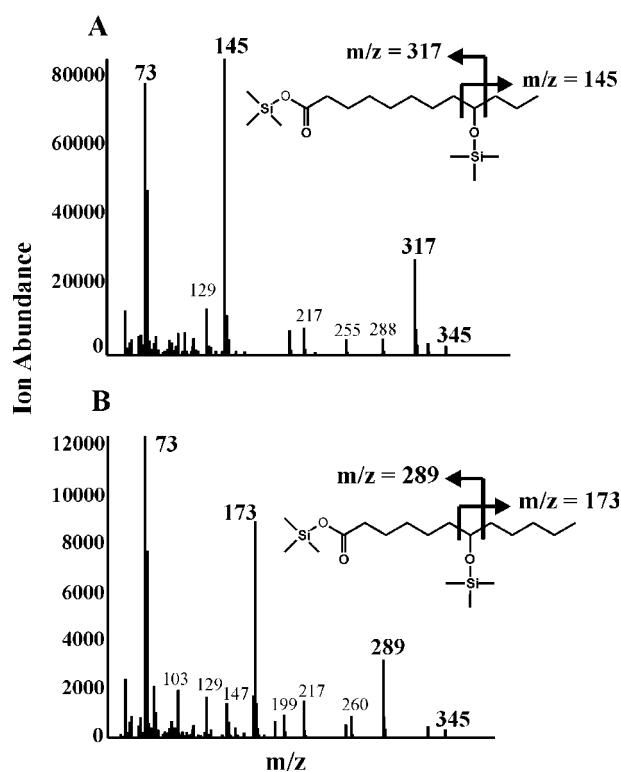


**Figure 2.** Representative mass spectrometry fragmentation patterns for the TMS-derivatized hydroxylated lauric acid peaks in Figure 1. **A)** MS fragments corresponding to the GC peak at 10.95 minutes, clearly identifying derivatized 9-hydroxylauric acid ( $\omega$ -3 hydroxylated product). **B)** MS fragments corresponding to the GC peak at 10.55 minutes, clearly identifying derivatized 7-hydroxylauric acid ( $\omega$ -5 hydroxylated product).

of H<sub>2</sub>O<sub>2</sub> or the lack of dependence on electron and proton transfer to the active site for formation of the reactive intermediate(s), two processes which are likely to coincide with conformational fluctuations that affect regioselectivity.

Peroxygenase reactions were initiated by addition of 10 mM H<sub>2</sub>O<sub>2</sub> and were extremely slow relative to hydroxylation *via* the natural pathway. These reactions require functional enzyme. In control experiments, reactions of free hemein chloride or heat-inactivated P450 with lauric acid in the presence of H<sub>2</sub>O<sub>2</sub> were shown to produce no oxidized fatty acid products. Wild-type (both full-length BM-3 and heme domain) is capable of no more than a few turnovers before it is inactivated, and inactivation is greatly accelerated by the presence of substrate (data not shown). The F87A mutant is more active than wild-type with H<sub>2</sub>O<sub>2</sub>, although inactivation still appears to be largely due to a competing, turnover-dependent reaction (data not shown). Similar observations have been made,[7] and the mechanism is currently under study. The full-length F87A mutant is reported to have an apparent K<sub>m</sub> for H<sub>2</sub>O<sub>2</sub> of ~18 mM,[7] in good agreement with our findings

(not shown). Higher concentrations of  $\text{H}_2\text{O}_2$  result in higher reaction rates, but the enzyme is also inactivated much faster. Even in 10 mM  $\text{H}_2\text{O}_2$  the enzyme is quickly inactivated: total turnovers for the F87A mutant are approximately 70 with lauric acid and 200 with capric acid. Shunt pathway reaction rates with myristic acid could not be quantified with high accuracy because there was no good authentic standard available for calibration (see Experimental Section). However, product peak areas show that the F87A mutant made 10–15 times more hydroxylated product than wild-type in one minute, implying a rate of  $\sim 20 \text{ min}^{-1}$ .

There appears to be a correlation between NADPH uncoupling and shunt pathway activity. The rate of the F87A shunt pathway with capric acid in 10 mM  $\text{H}_2\text{O}_2$  is in fact higher than the highly uncoupled F87A NADPH-driven reaction, and about the same as the wild-type NADPH-driven reaction (also highly uncoupled). This correlation between peroxygenase activity and uncoupling might be explained by increased hydrophilicity in the active site. The F87A mutation is likely to create space that permits more water molecules in the active site pocket. Poorer substrates are less effective at excluding water from the active site upon binding. Water remaining after substrate binding could promote  $\text{H}_2\text{O}_2$  access to the active site. Similarly, the presence of water could facilitate the dissociation of hydrogen peroxide anion from heme intermediates during NADPH-driven catalysis.<sup>[18]</sup>

We have quantified and compared the product distributions from NADPH- and  $\text{H}_2\text{O}_2$ -driven hydroxylation reactions of purified P450 BM-3 with fatty acids. That the product profiles from these different pathways are so similar suggests that we can harness peroxygenase activity without sacrificing P450 reaction specificity. Using the heme domain alone further simplifies this catalyst. However, wild-type P450 BM-3 is very slow and subject to rapid inactivation when it uses  $\text{H}_2\text{O}_2$ . Mutating Phe87 to a smaller residue increases this activity and provides a much improved starting point for further directed evolution to create a practical peroxide-driven hydroxylation catalyst.

## Experimental Section

### General Remarks

All chemical reagents were procured from Aldrich, Sigma, or Fluka.  $\text{H}_2\text{O}_2$  was purchased as a 35 wt % solution (Aldrich). NADPH (tetrasodium salt) was purchased from BioCatalytics, Inc. (Pasadena, CA). Fatty acids were added to reaction mixtures as 25–50 mM stock solutions of the sodium salts, which were prepared fresh each day in 50 mM  $\text{Na}_2\text{CO}_3$  and stored at 80 °C.  $\text{H}_2\text{O}_2$  and NADPH stock solutions were prepared fresh each day in 100 mM Tris-HCl, pH 8.2.

### Enzyme Expression and Purification

All enzymes (BWT, HWT, BFA, and HFA) were expressed in catalase-deficient *E. coli*<sup>[19]</sup> using the isopropyl- $\beta$ -D-thiogalactopyranoside (IPTG)-inducible pCWori(+) vector,<sup>[20]</sup> which is under the control of the double Ptac promoter. Heme domain only sequences (HWT and HFA) included a 6-His tag at the C-terminus, which had no noticeable effect on activity. Expression was accomplished by growth in terrific broth (TB) supplemented with 0.5 mM thiamine and trace elements.<sup>[21]</sup> Cultures were shaken at 150 rpm and 35 °C, induced after 9 hours by the addition of 1 mM  $\delta$ -aminolevulinic acid and 0.5 mM IPTG, and grown for an additional 22 hours at 100 rpm and 35 °C.

Purification of full-length enzymes (BWT and BFA) was performed essentially as described<sup>[22]</sup> using an Äkta explorer system (Pharmacia Biotech) and SuperQ-650M column packing (Toyopearl). Purification of the heme domain enzymes took advantage of the 6-His tag using the QIAexpressionist kit (Qiagen) for purification under native conditions. Briefly, cultures were grown as described above, and after centrifugation and resuspension in lysis buffer (10 mM imidazole, 50 mM  $\text{NaH}_2\text{PO}_4$ , pH 8.0, 300 mM NaCl) the cells were lysed by sonication. Cell lysates were centrifuged, filtered, and loaded onto a Qiagen Ni-NTA column. The column was washed with wash buffer (20 mM imidazole, 50 mM  $\text{NaH}_2\text{PO}_4$ , pH 8.0, 300 mM NaCl), and the bound P450 was eluted with elution buffer (200 mM imidazole, 50 mM  $\text{NaH}_2\text{PO}_4$ , pH 8.0, 300 mM NaCl). Aliquots of the purified proteins were placed into liquid nitrogen and stored at  $-80$  °C. When used, the frozen aliquots were rapidly thawed and buffer-exchanged with 100 mM Tris-HCl, pH 8.2 using a PD-10 Desalting column (Amersham Pharmacia Biotech). P450 enzyme concentrations were quantified by CO-binding difference spectra of the reduced heme as described,<sup>[23]</sup> using an extinction coefficient of  $91 \text{ mM}^{-1} \text{ cm}^{-1}$  for the 450 nm minus 490 nm peak.

### Determination of Product Distributions

Reactions contained purified P450 (1  $\mu\text{M}$  for the NADPH-driven reactions, 4  $\mu\text{M}$  for the  $\text{H}_2\text{O}_2$ -driven reactions) and 1–2 mM substrate in 500  $\mu\text{L}$  100 mM Tris-HCl, pH 8.2. Reactions were initiated by addition of either 2 mM NADPH or 10 mM  $\text{H}_2\text{O}_2$  and stopped by the addition of 7.5  $\mu\text{L}$  6 M HCl. At the end of each reaction an internal standard was added prior to extraction. For reactions with myristic and lauric acid, 30 nmoles of 10-hydroxycapric acid were used as the internal standard. For reactions with capric acid, 30 nmoles of 12-hydroxylauric acid were added as the internal standard.

Reactions were extracted twice with 1 mL ethyl acetate. The ethyl acetate layer was dried with sodium sulfate and then evaporated to dryness in a vacuum centrifuge. The resulting product residue was dissolved in 100  $\mu\text{L}$  of a 1:1 pyridine:BSTFA [bis(trimethylsilyl)trifluoroacetamide]] mixture containing 1% trimethylchlorosilane (TMCS). This mixture was heated at 80 °C for 30 minutes to allow for complete derivatization of the acid and alcohol groups to their respective trimethylsilyl (TMS) esters and ethers.

Reaction products were identified by GC/MS using a Hewlett Packard 5890 Series II gas chromatograph coupled with a Hewlett Packard 5989A mass spectrometer. MS fragmentation patterns clearly identified the hydroxylated

isomers. Quantification of the reaction products was accomplished using a Hewlett Packard 5890 Series II Plus gas chromatograph equipped with a flame ionization detector (FID). The GCs were fitted with an HP-5 column. The peak areas from each GC trace were normalized by dividing by the peak area of the internal standard. Authentic standards for each hydroxylated isomer of the fatty acids were not available, so standard curves were generated using the available  $\omega$ -hydroxylated standards (12-hydroxylauric acid and 10-hydroxycapric acid). Authentic standard samples were prepared in the same fashion as the reaction samples, except the standards were added to the reaction mixture and the enzyme was inactivated by the addition of HCl before adding NADPH or  $H_2O_2$ . It was assumed that the FID response is the same for all regioisomers of a given hydroxylated fatty acid. The standard curves were linear in the range of product detection, with R-squared values of 0.99 for the linear regression fits. A standard curve for hydroxylated myristic acid was prepared using  $\beta$ -hydroxymyristic acid, but there was significant loss of this standard during sample work-up compared to the reaction products and the resulting calibration curve was not used for quantifying hydroxylated products.

#### Determination of $H_2O_2$ -Driven Reaction Rates

Reactions were prepared as described above and stopped after 1 minute by the addition of 7.5  $\mu$ L 6 M HCl. Samples were treated as described above. Products were quantified by adding up all normalized FID product peaks and calculating the corresponding total hydroxylated product concentration from the  $\omega$ -hydroxylated standard curve.

#### Determination of NADPH-Driven Reaction Rates

Rates of NADPH-driven reactions were determined from initial rates of NADPH consumption. Reactions contained purified P450 (1  $\mu$ M for reactions with myristic and lauric acid and 3  $\mu$ M for reactions with capric acid) and 0.5–1 mM substrate in 100 mM Tris-HCl, pH 8.2 in a quartz cuvette. Reactions were initiated by addition of 0.2 mM NADPH and the initial rate of NADPH consumption was determined by measuring the decrease in absorbance at 340 nm, using an extinction coefficient of 6.2  $\text{mM}^{-1} \text{cm}^{-1}$ .<sup>[10]</sup> The background level of NADPH consumption (i.e., with no substrate present) was determined for wild-type ( $\sim 10 \text{ min}^{-1}$ ) and the F87A mutant ( $\sim 9 \text{ min}^{-1}$ ) and subtracted from the NADPH consumption rates.

#### Determination of Coupling Efficiency

Coupling efficiencies for NADPH-driven reactions with lauric acid and capric acid were determined by measuring the moles of product formed per 100 moles of NADPH consumed. Reactions (500  $\mu$ L) containing 1–2  $\mu$ M P450 and 2 mM substrate in 100 mM Tris-HCl (pH 8.2) were initiated by addition of 100  $\mu$ M (50 nmoles) NADPH and allowed to react to NADPH depletion. Products were then quantified from these reactions as described above.

## Acknowledgements

We thank Dr. Ulrich Schwaneberg and Dr. Edgardo Farinas for helpful advice and assistance and Dr. Nathan Dalleska for assistance with the GC procedures. This work was supported by the Biotechnology Research and Development Corporation (Peoria, IL).

## References

- [1] a) T. Sakaki, K. Inouye, *J. Biosci. Bioeng.* **2000**, *90*, 583; b) C. S. Miles, T. W. B. Ost, M. A. Noble, A. W. Munro, S. K. Chapman, *Biochim. Biophys. Acta-Protein Struct. Molec. Enzym.* **2000**, *1543*, 383; c) H. L. Holland, H. K. Weber, *Curr. Opin. Biotechnol.* **2000**, *11*, 547; d) M. Hara, *Mater. Sci. Eng. C-Biomimetic Supramol. Syst.* **2000**, *12*, 103.
- [2] F. P. Guengerich, *Nat. Rev. Drug Discov.* **2002**, *1*, 359.
- [3] H. Joo, Z. Lin, F. H. Arnold, *Nature* **1999**, *399*, 670.
- [4] R. T. Ruettinger, L. P. Wen, A. J. Fulco, *J. Biol. Chem.* **1989**, *264*, 10987.
- [5] Y. Miura, A. J. Fulco, *Biochim. Biophys. Acta* **1975**, *388*, 305.
- [6] H. Li, T. L. Poulos, *Biochim. Biophys. Acta* **1999**, *1441*, 141.
- [7] Q. S. Li, J. Ogawa, S. Shimizu, *Biochem. Biophys. Res. Commun.* **2001**, *280*, 1258.
- [8] a) U. Schwaneberg, C. Schmidt-Dannert, J. Schmitt, R. D. Schmid, *Anal. Biochem.* **1999**, *269*, 359; b) U. Schwaneberg, C. Otey, P. C. Cirino, E. Farinas, F. H. Arnold, *J. Biomol. Screen.* **2001**, *6*, 111.
- [9] a) X. Fang, J. R. Halpert, *Drug Metab. Dispos.* **1996**, *24*, 1282; b) I. Sevioukova, G. Truan, J. A. Peterson, *Arch. Biochem. Biophys.* **1997**, *340*, 231; c) O. Lentz, L. I. Qing-Shang, U. Schwaneberg, S. Lutz-Wahl, P. Fischer, R. D. Schmid, *J. Mol. Catal. B: Enzym.* **2001**, *15*, 123.
- [10] H. Yeom, S. G. Sligar, *Arch. Biochem. Biophys.* **1997**, *337*, 209.
- [11] a) S. S. Boddupalli, R. W. Estabrook, J. A. Peterson, *J. Biol. Chem.* **1990**, *265*, 4233; b) S. D. Black, M. H. Linger, L. C. Freck, S. Kazemi, J. A. Galbraith, *Arch. Biochem. Biophys.* **1994**, *310*, 126.
- [12] L. A. Cowart, J. R. Falck, J. H. Capdevila, *Arch. Biochem. Biophys.* **2001**, *387*, 117.
- [13] C. F. Oliver, S. Modi, M. J. Sutcliffe, W. U. Primrose, L. Y. Lian, G. C. Roberts, *Biochemistry* **1997**, *36*, 1567.
- [14] S. Graham-Lorence, G. Truan, J. A. Peterson, J. R. Falck, S. Wei, C. Helvig, J. H. Capdevila, *J. Biol. Chem.* **1997**, *272*, 1127.
- [15] P. R. Ortiz de Montellano, in *Cytochrome P450: Structure, Mechanism, and Biochemistry*, 2nd edn., (Ed.: P. R. Ortiz de Montellano), Plenum Press, New York, **1995**, pp. 245.
- [16] a) A. Ellin, S. Orrenius, *FEBS Lett.* **1975**, *50*, 378; b) J. Capdevila, R. W. Estabrook, R. A. Prough, *Arch. Biochem. Biophys.* **1980**, *200*, 186; c) P. Hlavica, I. Golly, J. Mietaschk, *Biochem. J.* **1983**, *212*, 539.

- [17] a) R. Renneberg, F. W. Scheller, K. Ruckpaul, J. Pirrwitz, P. Mohr, *FEBS Lett.* **1978**, *96*, 349; b) R. Renneberg, *Biochem. Pharmacol.* **1981**, *30*, 843; c) R. W. Estabrook, C. Martin-Wixtrom, Y. Saeki, R. Renneberg, A. Hildebrandt, J. Werringloer, *Xenobiotica* **1984**, *14*, 87; d) K. A. Holm, R. J. Engell, D. Kupfer, *Arch. Biochem. Biophys.* **1985**, *1985*, 477.
- [18] E. J. Mueller, P. J. Loida, S. G. Sligar, in *Cytochrome P450 Structure, Mechanism, and Biochemistry*, 2nd edn., (Ed.: P. R. Ortiz de Montellano), Plenum Press, New York, **1995**, pp. 83.
- [19] S. Nakagawa, S. Ishino, S. Teshiba, *Biosci. Biotechnol. Biochem.* **1996**, *60*, 415.
- [20] H. J. Barnes, M. P. Arlotto, M. R. Waterman, *Proc. Natl. Acad. Sci. USA* **1991**, *88*, 5597.
- [21] H. Joo, A. Arisawa, Z. Lin, F. H. Arnold, *Chem. Biol.* **1999**, *6*, 699.
- [22] U. Schwaneberg, A. Sprauer, C. Schmidt-Dannert, R. D. Schmid, *J. Chromatogr. A* **1999**, *848*, 149.
- [23] T. Omura, R. J. Sato, *J. Biol. Chem.* **1964**, *239*, 2370.
-